

1 **SWAT model-based quantification of the impact of land use change on sediment yield in the**  
2 **Fincha watershed, Ethiopia**

3

4 Motuma Shiferaw Regasa<sup>1</sup>, Michael Nones<sup>2,\*</sup>

5

6 <sup>1</sup> Department of Hydrology and Hydrodynamics, Institute of Geophysics, Polish Academy of Science, Warsaw,  
7 Poland; Ksiecia Janusza 64, 01-452 Warsaw, Poland; e-mail: mregasa@igf.edu.pl; ORCID 0000-0002-6955-6838

8 <sup>2</sup> Department of Hydrology and Hydrodynamics, Institute of Geophysics, Polish Academy of Science, Warsaw,  
9 Poland; Ksiecia Janusza 64, 01-452 Warsaw, Poland; phone: +48226915776; e-mail: mnonnes@igf.edu.pl; ORCID  
10 0000-0003-4395-2637 (author for correspondence)

11

12 The present version represents a non-peer reviewed preprint submitted to EarthArXiv.

13 In October 2022, this manuscript was submitted for consideration in CATENA (Elsevier).

14

15 **Abstract**

16 In recent years, Ethiopia is facing problems due to soil erosion, mainly because of the conversion  
17 of natural vegetation cover into cultivated land. Soil erosion is also affecting dam reservoirs, which  
18 are threatened by an increase in sediment yield entering the lake. The present study focuses on the  
19 Ethiopian Fincha watershed and takes advantage of the potentiality of SWAT, to investigate how  
20 land use land cover changes impact soil erosion and the consequent sediment yield entering the  
21 Fincha Dam, eventually suggesting potential management strategies. The SWAT model was  
22 calibrated and validated using time series data of stream flow and sediment from 1986 – 2008  
23 years, and its performance was evaluated by looking at the coefficient of determination, Nash-  
24 Sutcliffe simulation efficiency, and per cent bias. Once validated, the SWAT model was applied  
25 to derive sediment yield for the future thirty years, based on forecasted land use land cover

26 conditions. The results show that the mean annual soil loss rate increased from 32.51 t ha<sup>-1</sup> in 1989  
27 to 34.05 t ha<sup>-1</sup> in 2004, reaching 41.20 t ha<sup>-1</sup> in 2019. For the future, a higher erosion risk should  
28 be expected, with the annual soil loss rate forecasted to be 46.20 t ha<sup>-1</sup> in 2030, 51.19 t ha<sup>-1</sup> in 2040,  
29 and 53.98 t ha<sup>-1</sup> in 2050. This soil erosion means that sediments transported to the Fincha Dam,  
30 located at the watershed outlet, increased significantly in the last thirty years (from 1.44 in 1989  
31 to 2.75 mil t in 2019) and will have the same trend in the future (3.08 to 4.42 mil t in 2019 and  
32 2050, respectively), therefore highly affecting the Fincha reservoir services in terms of reduction  
33 of water volume for irrigation and hydroelectric power generation.

34

### 35 **Keywords**

36 Ethiopia; Fincha watershed; land use land cover; sediment yield; SWAT

37

### 38 **1. Introduction**

39 Changes in land use land cover (LULC) can cause soil erosion, which eventually contributes to  
40 increasing the quantity of sediments entering waterbodies and dam reservoirs. This process is  
41 evident in arid and semi-arid environments (Sharma et al., 2022), where soil degradation can  
42 generate cascading effects like poor conditions and famine (Yesuf et al., 2015). To counteract the  
43 erosion process and guarantee suitable development, effective management strategies and policies,  
44 and implementation of best management practices with the active involvement of all stakeholders  
45 are needed. However, to adopt adequate soil conservation measures, the extent and rate of soil  
46 erosion, as well as the causes of land degradation, must be assessed via the most appropriate  
47 modelling approach.

48 Nowadays, the Ethiopian economy and population are taking advantage of the presence of multiple  
49 dams and reservoirs, providing the availability of a large amount of water resources and suitable  
50 topography (Assfaw, 2019). However, these reservoirs are highly impacted by soil erosion, with  
51 consequent severe problems of sedimentation even beyond their dead storage capacity, which is a  
52 clear sign of poor land use practices and improper land management. Many studies pointed out  
53 that capacity to inflow ratio, amount of sediment flowing into the water, size and texture of the  
54 sediment, basin trap efficiency, reservoir operation methods, nature of the soil in the catchment  
55 area, basin topography, land use and vegetation cover in the catchment area and rainfall intensity  
56 are the main causes for sedimentation (Kumar et al., 2012; Foteh et al., 2018; Ivanoski et al., 2019).  
57 The reduction of storage volume due to sedimentation negatively impacts the capacity to produce  
58 hydroelectric power, increasing production and maintenance costs, reducing the availability of  
59 water for concurrent uses like irrigation, and eventually shortening the reservoir life.

60 Past investigations have shown a large variety of hydrological models used for evaluating and  
61 predicting soil erosion in Ethiopian watersheds, but most of them used the Soil and Water  
62 Assessment Tool (SWAT) (see, among many others, Gessese & Yonas, 2008; Senti et al., 2014;  
63 Yesuf et al., 2015; Ehabu et al.2019; Megersa et al., 2019; Mariye et al., 2022; Gebretekle et al.,  
64 2022). These studies confirmed that poor land use practices, improper land management and  
65 absence of appropriate soil conservation measures have been major causes of soil erosion and land  
66 degradation problems, with consequent sedimentation in Ethiopian reservoirs (Tefera et al.2010;  
67 Ayana et al.2012; Dibaba et al.2021).

68 During the past decades, the Fincha watershed, part of the Blue Nile River basin, has experienced  
69 dynamic LULC changes in the degradation of natural woodlands (Dibaba et al., 2021; Regasa et  
70 al., 2021). According to Leta et al. (2021) and Kenea et al. (2021), such LULC variations can have

71 both long- and short-term temporal and spatial effects on the watershed hydrology, and  
72 consequently on the soil erosion and sediment yield entering the dam reservoirs located in the  
73 watershed (Dibaba et al., 2021b).

74 The present investigation aims to evaluate the impact of LULC change on sediment yield entering  
75 the Fincha reservoir, looking at past trends (1989, 2004, 2019 years) and predicting future  
76 scenarios (2030, 2040, 2050 years). LULC scenarios were developed based on historical data and  
77 future predictions (Regasa & Nones, 2022) while hydrological changes and consequent sediment  
78 yield were computed by applying the SWAT model, given its reliability in modelling water and  
79 sediment loading (Gassman et al., 2007). The present findings contribute to a better understanding  
80 of soil erosion processes and consequences in a poorly gauged basin, giving useful insights on  
81 future management strategies and mitigation measures that can be applied for reducing sediments  
82 entering the Fincha reservoir, eventually contributing to assuring a longer service life.

83

## 84 **2. Materials and Methods**

### 85 ***2.1 SWAT model description***

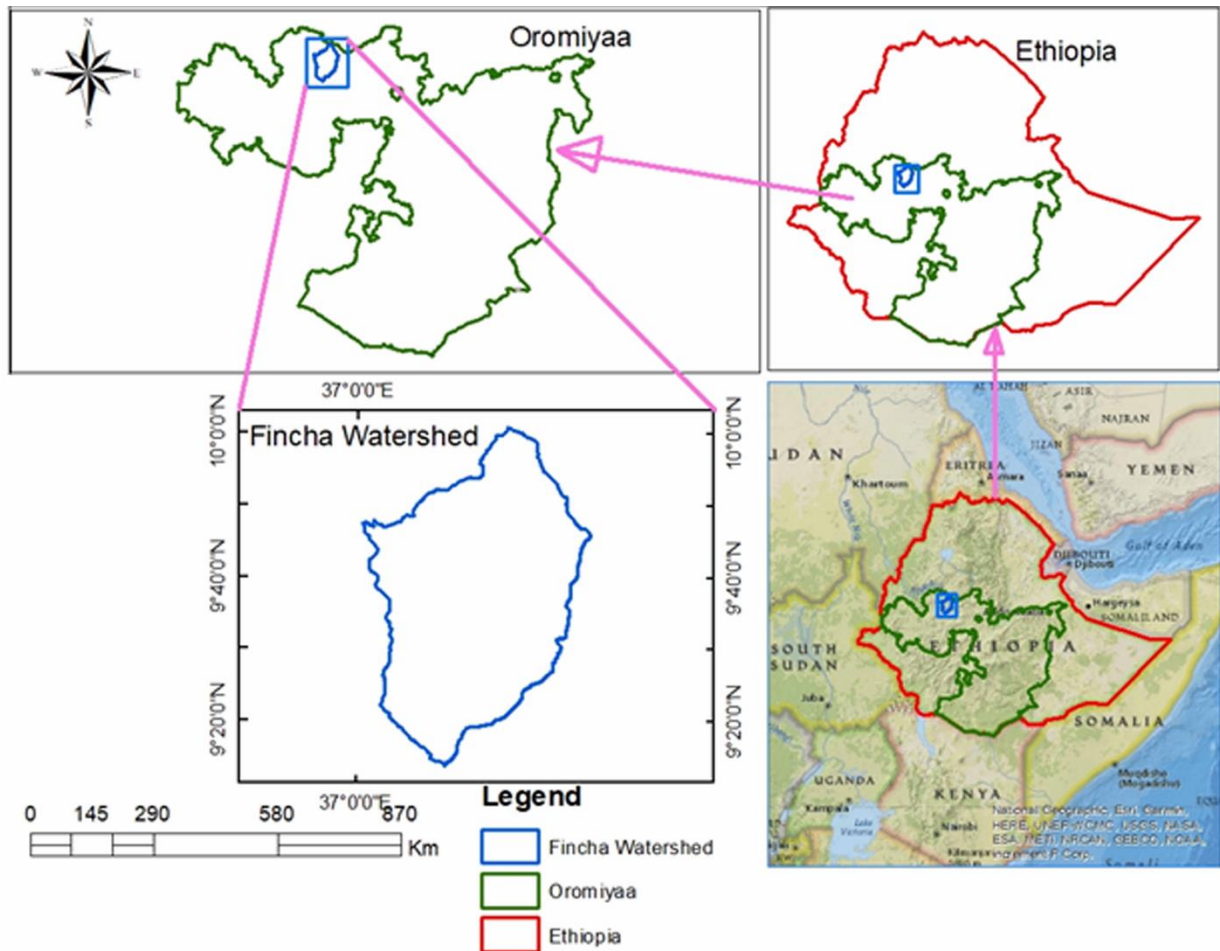
86 The Soil and Water Assessment Tool (SWAT) was developed by the United States Department of  
87 Agriculture (USDA), and is a continuous-time, semi-distributed, process-based watershed model.  
88 SWAT was initially developed to predict the impact of land management practices on water,  
89 sediment and chemical yields in agricultural watersheds (Arnold et al., 1998; Winchell et al., 2007)  
90 but, since then, it has been widely used to understand the hydrological cycle in general, simulating  
91 the effect of land use hydrology, water quality and ecosystem services, to eventually derive  
92 sediment yield and soil management practices (e.g., Qiu et al., 2014; Xue et al. 2014; Dibaba et al.  
93 2021; Kenea et al., 2021; Lin et al., 2022). There is ample literature proving the validity of SWAT

94 in modelling soil erosion and transport processes (e.g., Setegn et al., 2010; Phuong et al. 2014;  
95 Cousino et al. 2015; Djebou et al. 2018; Dakhlalla & Parajuli, 2019; Khanchoul et al. 2020).  
96 SWAT divides a watershed into sub-watersheds, connected through a stream channel. Further,  
97 each sub-watershed is divided into Hydrologic Response Units (HRUs), which represent a unique  
98 combination of soil, land use and slope type in a sub-watershed (Arnold et al., 2012; Rathjens &  
99 Oppelt, 2012). In SWAT, hydrology and sediment are simulated at the HRU level, and then the  
100 outputs are summarized first at the sub-watershed level, and then at the watershed level, routing  
101 these quantities through the stream network (Neitsch et al., 2011). SWAT can account for that,  
102 simulating all the effects of soil erosion and climate change on water supply properly (Krysanova  
103 & White, 2015).

104

## 105 ***2.2 Study Area***

106 The Fincha watershed is in Ethiopia's Horroo Guduruu Wallaggaa Oromiyaa regional state, in the  
107 Upper Blue Nile Basin, about 300 km from Addis Ababa. It is geographically located between  
108 latitudes 9°9'53" N to 10°1'00" N and longitudes 37°00'25" E to 37°33'17" E, as shown in the map  
109 (Figure 1).



110

111 Figure 1. Location of the Fincha watershed, Oromiyaa regional state, Ethiopia.

112

113 The region is defined by four distinct seasons: Summer, June to August, with heavy rains; Harvest  
 114 season occurs from September to November, winter, which lasts from December to February, is  
 115 illustrated by morning frost, particularly in January. Spring, from March to May, is the hottest  
 116 season, with showers on occasion. The annual rainfall in the study area ranges from 1367 to 1842  
 117 mm, with the Northern lowlands receiving the least rain and the Southern and Western highlands  
 118 receiving more than 1500 mm (Regasa and Nones, 2022). The main rainy season is from June to  
 119 September, where the average precipitation is around 1604 mm with peaks between July to August.

120 According to studies conducted by Regasa and Nones (2022) and Leta et al. (2021), natural  
 121 resources such as the Fincha, Amarti, and Nashe lakes not only contribute to the national economy  
 122 by generating hydroelectric power, but are also used to irrigate large sugar cane fields. Because of  
 123 its downstream connection to the Nile basin and intensive agriculture, the area is of national and  
 124 international interest in hydro politics.

125

126 **2.3 Available dataset**

127 The SWAT model requires multiple pieces of information, which come from different sources  
 128 (Table 1). In detail, the model inputs are Digital Elevation Model (DEM), LULC maps, soil data,  
 129 weather data (relative humidity, precipitation, solar radiation, temperature, and wind speed), water  
 130 flow and sediment data.

131

132 Table 1. Available data and sources.

<i>Type</i>	<i>Data</i>	<i>Resolution/year</i>	<i>Source</i>
Spatial Data	Digital elevation Model (DEM)	30m / 2019	Ministry of Water, Irrigation, Energy (MOWIE), Ethiopia
	Land use land cover	30m / 1989, 2004, 2019, 2030, 2040, 2050	1989, 2004, 2019 derived from Landsat images 2030, 2040, 2050 predicted by Land Change Modeler (Regasa & Nones, 2022)
	Soil		Ministry of Water, Irrigation and Energy (MOWIE), Ethiopia

Meteorologic al Data	Precipitation, Temperature, Relative humidity, Solar radiation, Wind speed	1986-2019 daily	Metrological National Agency, Ethiopia
Hydrological Data	Stream flow	1986-2008 daily	Ministry of Water, Irrigation, and Energy (MOWIE), Ethiopia
Sediment Data	Recorded sediment	1986-2008	Ministry of Water, Irrigation, and Energy (MOWIE), Ethiopia

133

134 *2.3.1 Meteorological data*

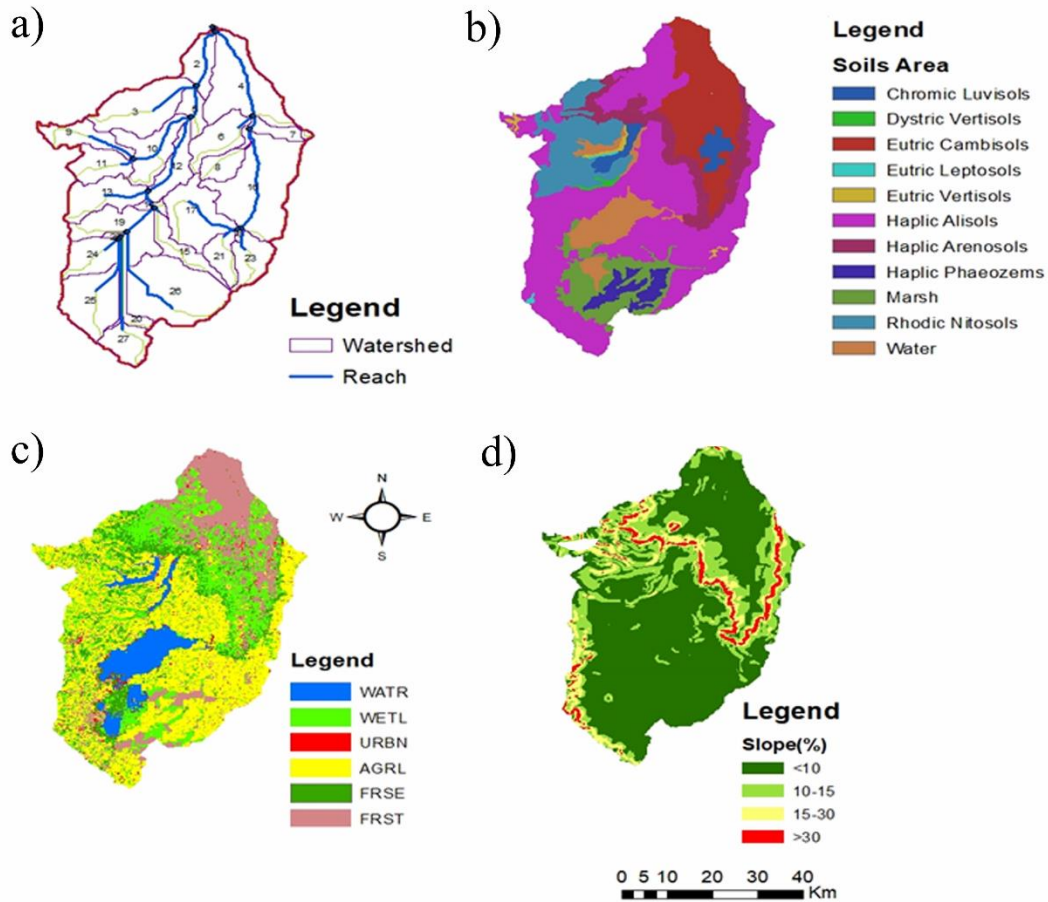
135 The analysis was performed using daily observed weather data covering the period 1986-2019  
136 years. These data include precipitations, maximum and minimum temperatures, solar radiation,  
137 wind speed and relative humidity, refer to ten gauging stations collected from the Ethiopian  
138 metrological agencies of are Alibo, Fincha, Gebete, Hareto, Homi, Jermet, Kombolcha, Nashe,  
139 Shambu and Wayyu. The statistical software *Xlstat* was used to fill gaps in the meteorological  
140 dataset.

141

142 *2.3.2 Soil data*

143 Soil information was obtained from the Ethiopian Ministry of Water, Irrigation and Energy  
144 (MOWIE), and they were pre-processed to follow the Food and Agricultural Organization (FAO)  
145 guidelines as stated in Pennock (2019). Ten soil types can be recognized in the Fincha watershed:  
146 Dystric Vertisols, Eutric Cambisols, Eutric Leptosols, Eutric Vertisols, Haplic Alisols, Haplic  
147 Arenosols, Haplic Phaeozems, Rhodic Nitisols, Chromic Luvisols, Water and Marsh (Figure 2b).





148

149 Figure 2. Main characteristics of the study area: a) river system and sub-watersheds; b) soil types;

150 c) LULC of 2019; d) terrain slope.

151

### 152 2.3.3 Land use land cover

153 Land use is a key SWAT model input that influences surface runoff, evapotranspiration, erosion,

154 nutrients and pesticide load in a watershed. The land use land cover (LULC) data used in the

155 present research were previously described by Regasa and Nones (2022), who investigated LULC

156 in past (1989, 2004, 2019) and future (2030, 2040, 2050) years. The area was classified into six

157 classes: waterbody, grass/swamp, built-up, agricultural land, forest, shrub (Figure 2c). The LULC

158 data set was reclassified into six major land classes as it is for use in SWAT. This reclassification

159 was conducted because the SWAT model needs standard names such as WATR, WETL, URBN,  
160 AGRL, FRSE and FRST for waterbody, grass/swamp, built-up, agricultural land, forest, and shrub  
161 respectively.

162

#### 163 *2.3.4 Slope*

164 Multiple slope classes were defined and then used to delineate SWAT HRU having the same slope,  
165 based on a 30m x 30m DEM of the Fincha watershed and using the Arc-GIS spatial analysis tool.  
166 When defining the hydrologic response unit, Arc-SWAT allows the integration of up to five slope  
167 classes. In addition, the SWAT model allows you to select a single or multiple slope class. As a  
168 result, the slope classes used in this study were broken down into four classes (10%, 15%, 25%,  
169 >30%) to represent the variation in the topography of the Fincha watershed (Figure 2d).

170

#### 171 *2.3.5 Sediment rating curve*

172 One of the most crucial pieces of information for estimating soil erosion in a hydrological study  
173 knows sediment characteristics. To overcome the lack of continuous measurements, a sediment  
174 rating curve was developed to relate daily stream flow to sediment data recorded at the outlet of  
175 the Fincha watershed. Such a curve can show how stream flow affects the rate of sediment  
176 movement (Assfaw, 2020), but its reliability high depends on the available dataset  
177 To simulate sediment yield and stream flow, SWAT needs, as model input, sediment, and stream  
178 flow data with a continuous time step. Due to the lack of continuous sediment data, these were  
179 derived by applying an empirical sediment rating curve to the simulated daily stream flow. Such  
180 an approach is generally used when there are few long-term and trustworthy records of sediment  
181 concentrations (Jilo et al., 2019).

182 Following literature evidence (e.g., Asselman, 2000; Horowitz, 2003; Franzoia & Nones, 2017,  
183 Assfaw, 2019), a general relationship between sediment concentrations and river discharge can be  
184 written as

$$185 \quad Q_s = aQ_f^b \quad (1)$$

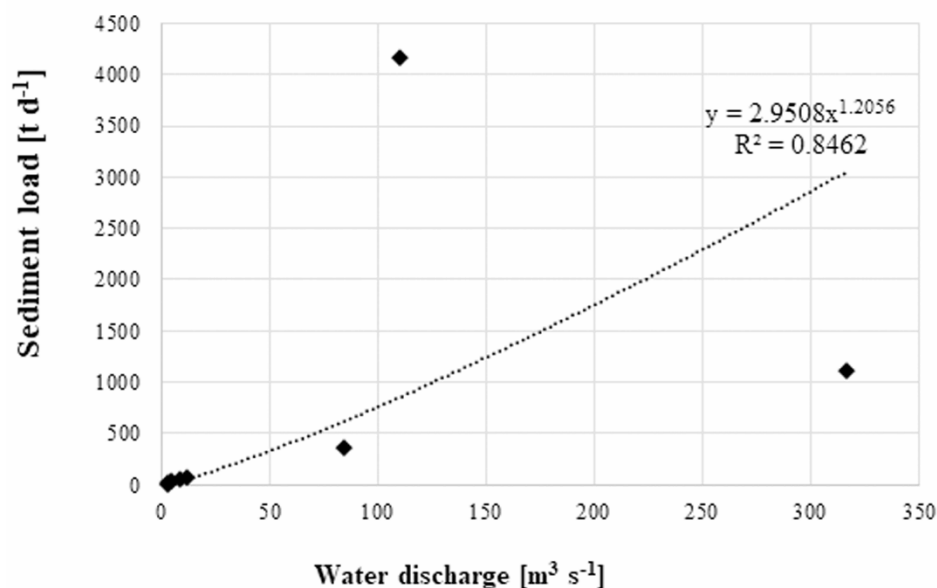
186 where  $Q_s$  is the sediment load in ton day<sup>-1</sup>,  $Q_f$  represents the stream flow in m<sup>3</sup> s<sup>-1</sup>, while  $a$  and  $b$   
187 are regression constants to be determined from a regression between measured sediment and water  
188 flows.

189 In the study case, the obtained sediment data was in mg l<sup>-1</sup>, but this concentration was converted  
190 to ton day<sup>-1</sup> via the equation

$$191 \quad Q_s = 0.0864 * C * Q_f \quad (2)$$

192 where  $C$  indicates the suspended sediment concentration (mg l<sup>-1</sup>)

193 Using the data obtained from MOWIE and reporting flow and sediment data measured at the  
194 Fincha gauging station between 1986 and 2008, a sediment rating was created (Figure 3). The  
195 regression constants  $a$  and  $b$  were found to be 2.9508 and 1.2056, respectively.



196

197 Figure 3. Sediment rating curve for the period 1986-2008. Data were measured at the Fincha  
198 gauging station (source: MOWIE).

199

#### 200 **2.4 SWAT model setup**

201 From the SWAT website (swat.tamu.edu), Arc-SWAT version 2012.10 4.19 was downloaded, and  
202 its interface was linked to Arc-GIS 10.3.1 for the modelling. This latter process involves setting  
203 up a SWAT project, defining the spatial extent of the analysis (watershed, sub-watersheds, HRUs),  
204 writing and editing SWAT input, and performing the simulations. Following the collection of data,  
205 all input data were prepared, the watershed and the HRUs were defined, and the classification of  
206 land use, soil, and slope was included in the model.

207 Based on the water balance equation (Swami and Kulkarni, 2016), SWAT simulates the  
208 hydrological cycle:

$$209 \quad SW_t = SW_o + \sum_{i=1}^t (R_{day} - Q_{surf} - E_a - W_{seep} - Q_{gw}) \quad (1)$$

210 where  $SW_t$  is the last soil water content (mm),  $SW_o$  is the first soil water content on day  $i$  (mm),  $t$   
211 indicates the time (days),  $R_{day}$  is the amount of precipitation on day  $i$  (mm),  $Q_{surf}$  represents the  
212 amount of surface runoff on day  $i$  (mm),  $W_{seep}$  is the amount of water entering vadose zone from  
213 the soil profile on day  $i$  (mm),  $E_a$  is the amount of evapotranspiration on day  $i$  (mm) and  $Q_{gw}$   
214 indicates the amount of return flow on day  $i$  (mm).

215 In our study, the SWAT model was applied to estimate, at the daily scale, hydrological components  
216 such as surface run-off, evapotranspiration, and sediment yield. Sediment yield was estimated at  
217 the HRU level, through a Modified Universal Soil Loss Equation (MUSLE) (Khelifa et al., 2016;  
218 Sahar et al., 2021)

$$219 \quad Sed = 11.8(Q_{surf} * q_{peak} * Area_{HRU})^2 * K * C * P * LS * CFRG \quad (2)$$

220 where  $Sed$  is sediment yield in metric tons per day,  $Q_{surf}$  is the surface runoff volume (mm),  $q_{peak}$   
221 is the peak run-off rate ( $m^3/s$ ),  $Area_{HRU}$  is the area of HRU (ha),  $K$  is the soil erodibility factor,  $C$   
222 is the cover and management factor,  $P$  is the practice support factor,  $LS$  is the topographic factor  
223 and  $CFRG$  is the course fragment factor.

224

#### 225 *2.4.1 Watershed delineation*

226 The watershed and the sub-watersheds were delineated by using the 30m-resolution DEM of the  
227 Fincha basin, via defining the stream network in SWAT and considering flow accumulation and  
228 water flow direction. SWAT models enable users to delineate watersheds and sub-watersheds  
229 using Digital Elevation Models (DEMs) by expanding the Arc-GIS and spatial analyst extension  
230 function. Watershed and sub-watershed delineation was accomplished through a series of steps,  
231 including DEM setup, stream definition, inlet outlet definition, watershed outlet selection and  
232 definition, and finally sub-basin parameter calculation (Figure 2a).

233 The Arc SWAT model interface by default proposes the minimum and maximum watershed area,  
234 as well as the size of the sub-watershed in hectares to define the minimum drainage area required  
235 to form the stream's origin. The smaller the threshold area, the more detail of the drainage network,  
236 the greater the number of sub-watersheds, and the higher the number of HRUs. However, more  
237 processing time and computer space are required. As a result, the model's proposed threshold was  
238 used to determine the optimal size of the threshold area as described in section 2.4.2 below.

239

#### 240 *2.4.2 Hydrologic Response Units*

241 HRUs were defined based on the topographical characteristics of the terrain as derived from the  
242 DEM and assigned to each sub-watershed based on a threshold value for LULC, soil, and slope

243 categories. According to Megersa et al., (2021), a threshold of 10% was imposed in defining  
244 HRUs, to exclude areas characterized by small land uses and slope classes. Consequently, the  
245 Fincha watershed was divided into 27 sub-watersheds and then subdivided into 234 HRUs. It is  
246 worth reminding that only 9 of these sub-watersheds are located upstream of the Fincha Dam, and  
247 are therefore contributing to the sediment yield entering the dam.

248

#### 249 *2.4.3 Model calibration and validation*

250 A sensitivity analysis is needed to investigate the model's capacity to adequately predict water  
251 stream flow and sediment yield (Anaba et al., 2016), and this was done via the SWAT Calibration  
252 and Uncertainty Procedures (SWAT-CUP) interface (Mekuriaw, 2019) combined with the SUFI-  
253 2 approach (Leta et al., 2021). SWAT Calibration and Uncertainty Procedures (SWAT-CUP), a  
254 program for integrated sensitivity analysis, calibration, and validations, were used to analyze the  
255 uncertainties of SWAT model prediction (Dibaba et al., 2021). In this investigation, the sensitivity  
256 analysis was performed using the SUFI-2 techniques and looking at the water discharge - sediment  
257 load data measured at the outlet of the Fincha Reservoir (at Fincha Dam) during the period 1986-  
258 2008.

259 To perform model calibration and validation, the stream flow and sediment data were divided into  
260 two periods, and an initial warm-up period was also taken into consideration. The initial three  
261 (1986-1988) years were chosen as the warm-up period, while the calibration was performed for  
262 the 1989-2002 years while 2003-2008 were utilized to validate the SWAT model.

263 To test the goodness of fit between monthly simulated and observed values, the model's  
264 performance was assessed using the coefficient of determination ( $R^2$ ), the Nash-Sutcliffe  
265 simulation efficiency ( $NSE$ ), and the per cent bias ( $PBIAS$ ).

266 Determination coefficients can range from 0 (inadequate model) to 1 (the model perfectly fits the  
 267 data), and, typically, values  $R^2$  larger than 0.6 indicate good correlation (Leta et al. 2021).

268 The  $NSE$  values can reach a maximum of 1 (perfect fit), while a negative  $NSE$  value indicates that  
 269 the model's performance is inferior to that obtained using the observations' mean as a predictor  
 270 (Jilo et al., 2019). The simulation efficiency is classified as unsatisfactory, satisfactory, good, or  
 271 very good if  $NSE < 0.50$ ,  $0.5 < NSE < 0.65$ ,  $0.65 < NSE < 0.75$ ,  $0.75 < NSE < 1$ , respectively (Leta et al.,  
 272 2021).

273  $PBIAS$  assesses the typical tendency of the simulated data to differ from the observed data in size  
 274 or frequency, and lower  $PBIAS$  values indicate better simulation results. Moriasi et al. (2007)  
 275 define  $PBIAS$  positive values as a model underestimation, while negative values as a model  
 276 overestimation.

277 According to Yasir et al. (2020) and Dibaba et al. (2021), the following equations were applied to  
 278 determine  $R^2$  (eq. 3),  $NSE$  (eq. 4) and  $PBIAS$  (eq. 5):

$$279 \quad R^2 = \left[ \frac{\sum_{i=1}^n (Q_{Obs} - \bar{Q}_{Obs})(Q_{Cal} - \bar{Q}_{Cal})}{\sum_{i=1}^n (Q_{Obs} - \bar{Q}_{Obs})^2 \sum_{i=1}^n (Q_{Cal} - \bar{Q}_{Cal})^2} \right]^2 \quad (3)$$

$$280 \quad A = 1 - \frac{\sum_{i=1}^n (Q_{Obs} - Q_{Cal})^2}{\sum_{i=1}^n (Q_{Obs} - \bar{Q}_{Obs})^2} \quad (4)$$

$$281 \quad PBIAS = \frac{\sum_{i=1}^n (Q_{Obs} - Q_{Cal}) * 100}{\sum_{i=1}^n Q_{Obs}} \quad (5)$$

282 where  $Q_{Obs}$  is the actual variable,  $\bar{Q}_{Obs}$  is the time average of the variable  $Q_{Obs}$ ,  $Q_{Cal}$  is the simulated  
 283 variable and  $\bar{Q}_{Cal}$  is its time average. It is worth noticing that these equations are valid for both  
 284 water flow and sediment data.

285

## 286 **2.5 Scenarios simulation**

287 Using scenario-based simulations, the effects of current and future LULC changes on watershed  
288 sediment yield were assessed for the period 1989-2050. This was done by creating six scenarios  
289 (historical reference years 1989, 2004, 2019; future predicted 2030, 2040, 2050) accounting for  
290 different LULC conditions (Regasa & Nones, 2022). A fixing-changing method was applied to  
291 investigate the effects of LULC change (Leta e al., 2021): SWAT was run with changing LULC  
292 maps, but all the other modelling parameters were kept constant as derived from the model  
293 validation (Gessesse et al., 2015). The sediment yield was computed separately for the entire  
294 Fincha watershed (27 sub-watersheds) and the region upstream of the Fincha Dam (9 sub-  
295 watersheds).

296 Pearson's correlation method (Aga et al., 2020) was used to assess the variations in LULC classes  
297 and the sediment yields, while the pair-wise Pearson correlation matrix was applied to detect linear  
298 correlations.

299

## 300 **3. Results**

### 301 **3.1 Sensitivity analysis**

302 A sensitivity analysis for the simulated stream flow and sediment was carried out to determine the  
303 most sensitive parameter with the greatest impact on model results. According to the SWAT  
304 manual and the literature (Khelifa et al., 2017, Yuan & Forshay, 2019, Daramola et al., 2019), nine  
305 (Table 2) and seven (Table 3) parameters for stream flow and sediment were respectively selected  
306 as the initial input for the model sensitivity analysis.

307 The sensitivity analysis was based on the SUFI-2 algorithm techniques (Arnold et al., 2013). The  
308  $p$ -value and the  $t$ -stat value were used to assess the sensitivity of each parameter and then rank it,



309 with rank 1 indicating the most sensitive parameter. Statistically, bigger absolute *t*-stats and lower  
 310 *p*-values mean that a parameter is significant. On the other part, a high *p*-value indicates that there  
 311 is no correlation between changes in the predictor values and the response variable (Pandey et al.,  
 312 2021).

313  
 314 Table 2. Stream flow parameters with range and fitted value, as derived from the sensitivity  
 315 analysis performed using SUFI-2. Their rank was established based on P-value.

Parameter Name	Description	Range	Fitted value	Calibration		
				<i>t</i> -stat	<i>p</i> -value	Rank
V_GW_DELAY. gw	Groundwater delay (days)	0 - 500	21.25	-9.891	0.000	1
R_CN2.mgt	SCS runoff curve number II	-25 - 25	-15.625	2.391	0.018	2
V_GWQMN.gw	Threshold depth of water in the shallow aquifer required for return flow to occur (mm H2O)	0 - 5000	2012.5	-2.022	0.045	3
R_CH_N2.rte	Manning's "n" value for the main channel	0 - 1	0.7575	0.717	0.474	4
R_SOL_AWC(1).sol	Available water capacity of the 1st	-25 - 25	6.875	0.699	0.486	5

	soil layer (mm H <sub>2</sub> O mm soil <sup>-1</sup> )					
R_SOL_K(1).sol	Saturated hydraulic conductivity at the 1st soil layer (mm h <sup>-1</sup> )	-25 - 25	9.875	0.255	0.799	6
R_SLSUBBSN.hr u	Average slope length (m)	0 - 150	133.875	0.153	0.878	7
R_RCHRГ_DP.g w	Deep aquifer percolation fraction	0 - 1	0.6475	- 0.099	0.921	8
V_ALPHA_BF.g w	Base flow alpha factor (1 day <sup>-1</sup> )	0 - 1	0.3125	0.060	0.952	9

316

317 Table 3. Sediment parameters with range and fitted value, as derived from the sensitivity analysis  
318 performed using SUFI-2. Their rank was established based on P-value.

Parameter Name	Description	Range	Fitted value	Calibration		
				t-stat	P value	Rank
R_SPEXP.bsn	Exponential factor for channel sediment routing	0 - 2	1.71	-9.85	0.00	1
R_LAT_SED.hru		1 - 1000	242.50	-5.07	0.00	2

R_CH_COV2.rte		0 - 1	0.56	-3.06	0.00	3
R_SPCON.bsn	linear factor for channel sediment routing	0 – 0.01	0.005	-1.95	0.05	4
R__CH_COV1.rte		0.01 – 0.06	0.11	-1.53	0.13	5
R__PSP.bsn	Peak rate adjustment factor for sediment routing in the sub- basin (tributary channels)	0 - 1	0.88	-0.42	0.67	6
R__USLE_P.mgt	USLE support Practice factor	0 - 1	0.208	-0.31	0.75	7

319

### 320 ***3.2 Calibration and validation***

321 Using the observed monthly stream flow and sediment at Fincha reservoir close to the Fincha Dam  
322 outlet from 1986 to 2008 years, the model parameters of SWAT were calibrated and validated.

323 The warm-up period 1986-1988 was used to reduce the impact of the model's initial conditions  
324 during the model's initial stage of operation, while the calibration period lasted from 1989 to 2002,  
325 and the validation period from 2003 to 2008.

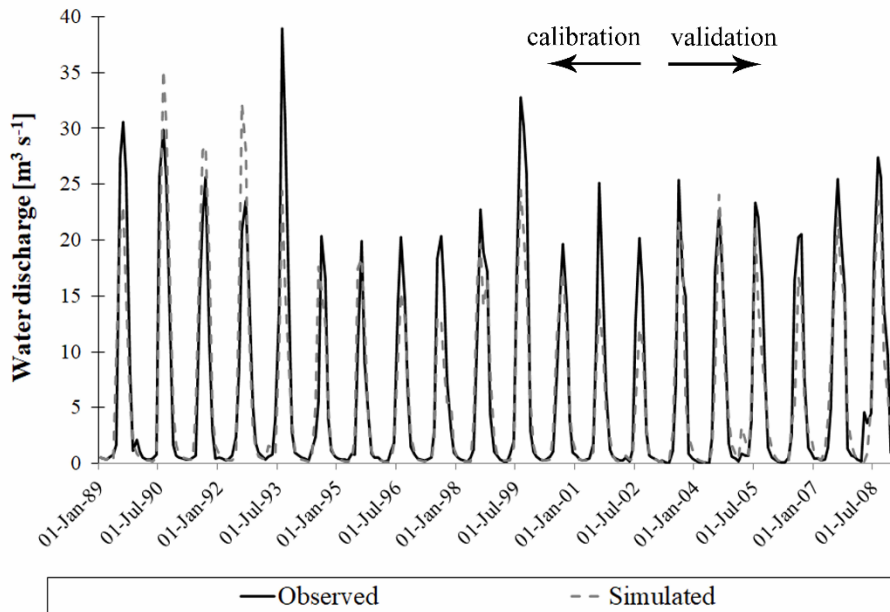
326 The model is very effective at simulating the stream flow (Figure 4), as shown by the values  
327 computed for the calibration and validation phases, summarized in Table.

328

329 Table 4. Simulation of water discharge: model performance during the calibration and validation  
 330 phases.

Statistical test	$R^2$	$NSE$	$PBIAS$
Calibration	0.83	0.83	8.3
Validation	0.84	0.76	12.2

331



332

333 Figure 4. Comparison between computed and measured water discharge at the Fincha Dam outlet,  
 334 during the calibration (1989-2002) and validation (2003-2008) phases.

335

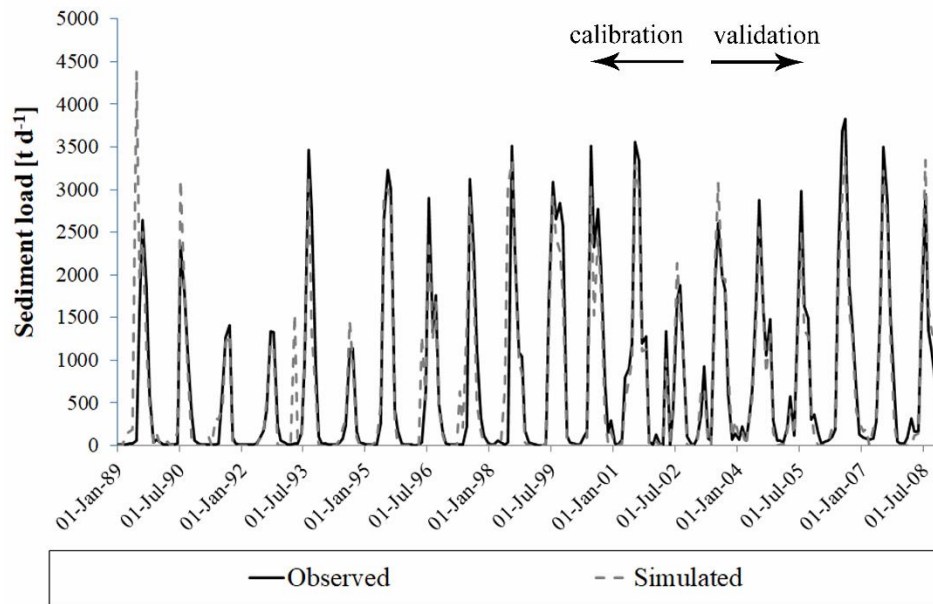
336 The SWAT model was also calibrated and validated in terms of monthly sediment transport (Table  
 337 5). A positive  $PBIAS$  for both periods indicates that the overall expected sediment production had  
 338 been underestimated, mainly due to problems in detecting sediment peaks (Figure 5).

339

340 Table 5. Simulation of sediment yield: model performance during the calibration and validation  
 341 phases.

Statistical test	$R^2$	$NSE$	$PBIAS$
Calibration	0.83	0.63	8.3
Validation	0.86	0.72	12.2

342



343

344 Figure 5. Comparison between computed and measured sediment load at the Fincha Dam outlet,  
 345 during the calibration (1989-2002) and validation (2003-2008) phases.

346

### 347 **3.3 Sediment yield estimation**

348 The SWAT model was applied to simulate sediment yield in 27 sub-watersheds (see Section 2.4.2).

349 Based on the approach proposed by Dibaba et al (2021), these sub-watersheds were classified in  
 350 terms of soil loss (Table 6).

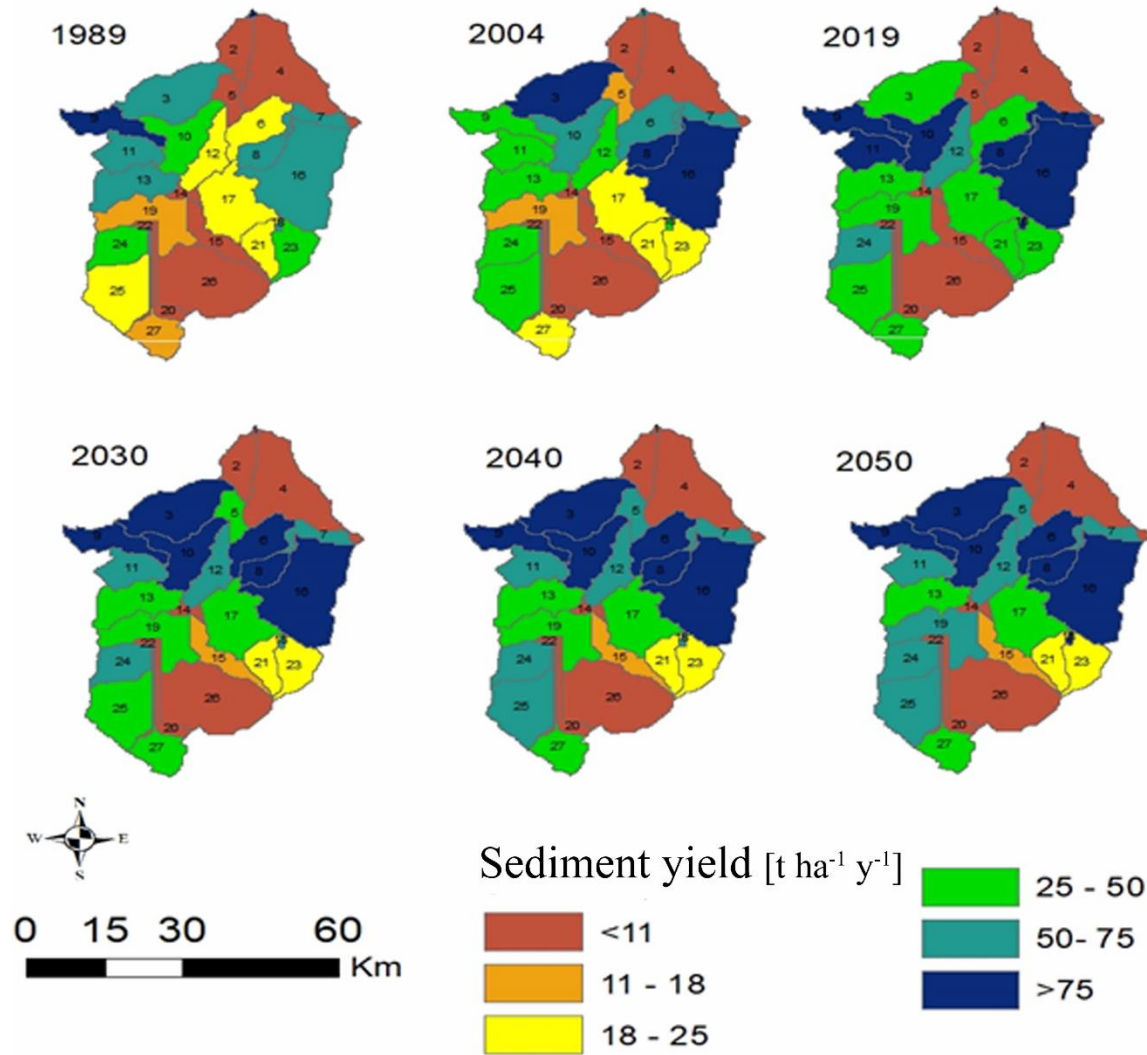
351

352 Table 6. Classification in terms of annual soil loss and severity.

Annual soil loss [t ha <sup>-1</sup> ]	Severity
<11	Low
11-18	Moderate
18-25	High
25-50	Very high
50-75	Severe
>75	Very severe

353

354 This classification pointed out significant dissimilarities across the Fincha watershed (Figure 6),  
355 which are mainly connected with the different LULC of each sub-watershed, as discussed in the  
356 next sections.



357

358 Figure 6. Spatial distribution of the sediment yield, subdivided for each sub-watershed.

359

360 The annual sediment yield in the Fincha watershed ranges from 0.36 to 83.74, from 0.80 to 113.72,

361 from 0.28 to 121.96, from 0.48 to 117.92, 1.06 to 162.96, from 1.12 to 183.80  $t\ ha^{-1}$  for 1989,

362 2004, 2019, 2030, 2040, 2050 scenarios, respectively. The annual average sediment yield was

363 computed as 32.51, 34.05, 41.20, 46.20, 51.19, 53.98  $t\ ha^{-1}$  for the same six scenarios, respectively,

364 meaning an increase of 8.69  $t\ ha^{-1}$  from 1989 to 2009, while the increase forecasted for the next 30

365 years (2019 to 2050) will be even more significant, reaching 12.78  $t\ ha^{-1}$ .

366 Focusing only on the nine sub-watersheds upstream of the Fincha Dam, and therefore contributing  
 367 to feeding the reservoir with sediments, the average annual sediment yield spans from 0.36 to  
 368 40.06, from 0.40 to 48.96, from 0.28 to 61.72, from 0.94 to 64.42, from 1.06 to 68.78 and from  
 369 1.12 to 69.96 t ha<sup>-1</sup> for 1989, 2004, 2019, 2030, 2040, 2050, respectively. The annual average  
 370 sediment yield for these scenarios is 6.71, 8.49, 12.30, 13.69, 14.57 and 15.19 t ha<sup>-1</sup>, respectively.  
 371 In Table 7 the results are summarized in terms of severity, showing an increase in areas affected  
 372 by high to very severe erosion.

373

374 Table 7. Annual soil erosion and its severity for past and future scenarios of Fincha reservoir

Year	Annual soil loss [t ha <sup>-1</sup> ]	Severity	Area [ha]	Area in per cent [%]
1989	<11	Low	14348.00	17.77
	11 – 18	Moderate	23132	28.64
	18 – 25	High	34044	42.16
	25 – 50	Very high	9232	11.43
	50 – 75	Severe	0	0.00
	>75	Very severe	0	0.00
2004	<11	Low	14348	17.77
	11 - 18	Moderate	14740	18.25
	18 - 25	High	25472	31.54
	25 - 50	Very high	26196	32.44
	50 - 75	Severe	0	0.00
	>75	Very severe	0	0.00



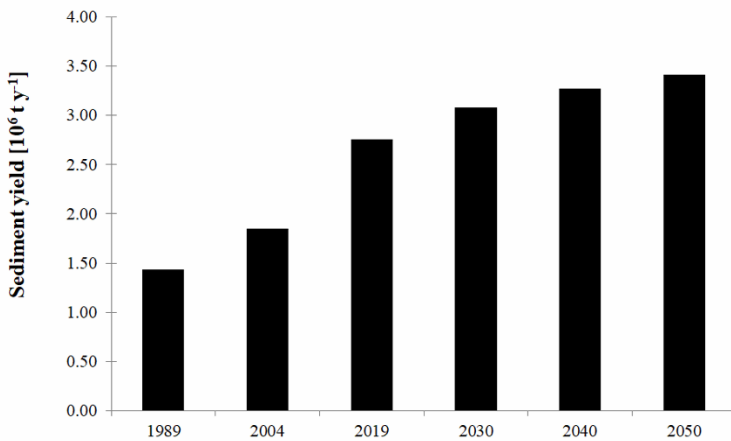
2019	<11	Low	14348	17.77
	11 - 18	Moderate	0	0.00
	18 - 25	High	0	0.00
	25 - 50	Very high	57176	70.80
	50 - 75	Severe	9232	11.43
	>75	Very severe	0	0.00
2030	<11	Low	6996	8.66
	11 - 18	Moderate	7352	9.10
	18 - 25	High	0	0.00
	25 - 50	Very high	57176	70.80
	50 - 75	Severe	9232	11.43
	>75	Very severe	0	0.00
2040	<11	Low	6996	8.66
	11 - 18	Moderate	7352	9.10
	18 - 25	High	0	0.00
	25 - 50	Very high	40212	49.79
	50 - 75	Severe	26196	32.44
	>75	Very severe	0	0.00
2050	<11	Low	6996	8.66
	11 - 18	Moderate	7352	9.10
	18 - 25	High	0	0.00
	25 - 50	Very high	25472	31.54
	50 - 75	Severe	40936	50.69

	>75	Very severe	0	0.00
--	-----	-------------	---	------

375

376 Even if the average annual sediment yield of sub-watersheds locates upstream of the Fincha Dam  
 377 is lower than the average annual sediment yield of the whole watershed, the sediment amount  
 378 entering annually the reservoir is still very high. In detail, 1.44, 1.85, 2.75, 3.08, 3.27, 3.42 mil t  
 379 in 1989, 2004, 2019, 2030, 2040, 2050, respectively, can enter the dam lake (Figure 7).

380



381

382 Figure 7. Annual sediment yield entering the Fincha Dam reservoir from the sub-watersheds  
 383 located upstream.

384

#### 385 4. Discussion

386 The observed and simulated water and sediment discharges at the Fincha Dam showed an overall  
 387 good agreement, indicating the reliability of the SWAT model in simulating these parameters in  
 388 data-scarce regions. However, the model was unable to adequately reproduce the peaks in both  
 389 water discharge and sediment yield. The underestimation of peak water flows generally results in  
 390 an underestimation of the sediment peaks (Akoko et al., 2021), and such an underestimation is also  
 391 a significant source of error in defining the overall sediment load of the watershed.

392 Moreover, the reliability of SWAT in estimating sediment yield is highly dependent on the  
393 availability of long-term datasets. In Ethiopia, long-term monitoring data are very rare, especially  
394 in terms of sediment information. To overcome this issue, in the present work a sediment rating  
395 curve characterized by a strong correlation ( $R^2=0.86$ ) between recorded sediment and water flow  
396 data was implied.

397 Based on this sediment rating curve, the annual soil loss was evaluated, as well as the areas  
398 characterized by a major soil loss (hotspots), eventually prioritizing management strategies in these  
399 zones. For the entire Fincha watershed, the mean annual soil loss rate was calculated as 32.51 t ha<sup>-1</sup>  
400 <sup>1</sup>, 34.05 t ha<sup>-1</sup>, 41.20 t ha<sup>-1</sup>, 46.20 t ha<sup>-1</sup>, 51.19 t ha<sup>-1</sup>, 53.98 t ha<sup>-1</sup> in 1989, 2004, 2019, 2030, 2040,  
401 2050, respectively. This translates into an increase of annual soil loss of 8.69 t ha<sup>-1</sup> during the last  
402 30 years (1989-2019), and a forecasted increase of 12.78 t ha<sup>-1</sup> for the next three decades, which  
403 will further negatively impact the overall basin as well as the reservoirs located therein.

404 As pointed out by Dibaba et al. (2021), tolerable soil loss is needed for maintaining ecosystem  
405 services without compromising the soil's ability to continue providing those services in the future.  
406 The maximum tolerable soil loss (0-11 t ha<sup>-1</sup> year<sup>-1</sup>) estimated for Ethiopian watersheds is much  
407 lower than the estimated mean annual soil loss rate in the current study area (Girmay et al., 2020;  
408 Ayalew et al., 2022), pointing out that the Fincha watershed is at very high of soil erosion. On the  
409 other part, the Fincha soil erosion rates are much lower than other local scale studies, which  
410 estimated an annual soil loss rate of 377.26 t ha<sup>-1</sup> in the Chogo watershed, located very close to  
411 the current study area (Negash et al., 2021).

412 The mean annual sediment yields of the nine sub-watersheds located upstream of the Fincha Dam  
413 span will increase from 13.42 t ha<sup>-1</sup> in 1989 to 30.38 t ha<sup>-1</sup> in 2050. As the estimated mean annual  
414 soil loss rate is considerably higher than the maximum tolerable soil loss limit of 11 t ha<sup>-1</sup>, also

415 this area is threatened by high erosion, with consequent negative effects on the socio-economy.  
416 More than 85% of the Ethiopian population depends on agriculture for living, therefore physical  
417 soil and nutrient losses can lead to food insecurity.

418 According to the estimated rates of mean annual soil loss, the erosion risk was classified into six  
419 classes (Table 6). The proportion of area at low erosion risk covered around 18% of the basin  
420 during the past (reference years 1989, 2004, 2019) while a decrease is forecasted for the future  
421 (around 9% in 2030, 2040, 2050). On the other part, areas exposed to high erosion risk will  
422 increase, mainly because of deforestation in favour of agricultural land, expansion of urban areas  
423 and grassland, growth and relocation of the population. This dynamic and rate of soil loss is a  
424 characteristic of many highland areas in Ethiopia (Weldu Woldemariam & Edo Harka, 2020),  
425 pointing out that the problem of soil erosion should be tackled at the national level, rather than  
426 with very local policies.

427 The soil erosion risk had shown a high spatial variation across the study landscape (Figure 6): low-  
428 risk areas were predicted downstream of the Fincha Dam, while areas characterized by the highest  
429 erosion risk are in the northwestern and eastern parts of the Fincha watershed.

430 Relatively less eroded areas were situated at lower elevations in the eastern and western parts of  
431 the sub-basin, where the slope inclination is below 10% with the above-mentioned factors made  
432 the area generate high soil loss risks. Similar results have been reported by earlier studies that  
433 directly correlated soil loss rate to terrain slope (Dibaba et al., 2021). According to Regasa et al.  
434 (2021), the communities displaced from the reservoir areas were forced to resettle downstream of  
435 the dam, in areas characterized by lower soil loss. However, these communities were forced to  
436 relocate without receiving fair compensation because of the expansion of the number and  
437 dimension of reservoirs for hydropower production, taking them away from their farmland (Dibaba

438 et al., 2020). Residents found it difficult to stay and were compelled to relocate due to the increased  
439 resettlement on unproductive lands and the relative depreciation of agricultural land, which results  
440 in further increasing soil erosion.

441 This study pointed out that all the sub-watersheds of the Fincha watershed are highly threatened  
442 by soil erosion, and therefore require management and mitigation strategies to safeguard the  
443 environment and reduce the sediment yield entering the Fincha reservoir. However, such strategies  
444 could be costly and time-consuming, and cannot be applied at the same time all over the watershed.  
445 In this respect, the present investigation can provide information on what areas should be  
446 prioritized, but more studies are needed to propose effective management strategies to reduce soil  
447 erosion that also account for the sustainable socioeconomic development of the area.

448

## 449 **5. Conclusions**

450 Using the Fincha watershed as a case study, the present research focused on understanding, via a  
451 modelling approach, the impact of LULC changes on soil erosion, comparing past trends with  
452 future predictions. It was found that the present LULC changes, which are favoring agricultural  
453 land and settlements over natural forests, have a detrimental impact on soil erosion, which  
454 increased from 32.51 t ha<sup>-1</sup> year<sup>-1</sup> in 1989 to 41.20 t ha<sup>-1</sup> year<sup>-1</sup> in 2019, and will increase till 53.98  
455 t ha<sup>-1</sup> year<sup>-1</sup> in 2050 at the watershed scale. Such soil loss translates into sediment yield transported  
456 in the Fincha Dam reservoir, which was estimated to increase from 1.44 mil t in 1989 to 3.42 mil  
457 t in 2050, eventually reducing the lifetime of the dam.

458 Based on the estimated rate of mean annual soil loss, the erosion risk was classified into six classes,  
459 pointing out that over 91% of the watershed is forecasted at high to severe erosion risk, with severe  
460 erosion located in the central, northeastern, and northwestern sub-watersheds. As soil erosion

461 represents a major threat to the current socio-economic development of the area, the classification  
462 proposed here could serve as a basis to prioritize future management strategies, aiming to reduce  
463 the impact of soil loss on the local environment and population.

464

#### 465 **Author Contributions**

466 Conceptualization, M.S.R. and M.N.; writing-original draft preparation, M.S.R. and M.N.;  
467 literature review, M.S.R. and M.N.; modelling, M.S.R.; data analysis, M.S.R.; supervision, M.N.;  
468 project administration, M.N.; funding acquisition, M.N.

469

#### 470 **Funding**

471 This research was funded by NCN National Science Centre Poland–call PRELUDIUM BIS-1,  
472 Grant Number 2019/35/O/ST10/00167. Project website: [https://sites.google.com/view/lulc-](https://sites.google.com/view/lulc-fincha/home)  
473 [fincha/home](https://sites.google.com/view/lulc-fincha/home).

474

#### 475 **Data availability**

476 The data used in the present research are available at the IG PAS Data Portal ([dataportal.igf.edu.pl](http://dataportal.igf.edu.pl))  
477 and from the corresponding author.

478

#### 479 **Reference**

480 Aga, A. O., Melesse, A. M., & Chane, B. (2020). An alternative empirical model to estimate  
481 watershed sediment yield based on hydrology and geomorphology of the basin in data-scarce  
482 rift valley lake regions, Ethiopia. *Geosciences*, 10(1), 31.

483 Akoko, G., Le, T. H., Gomi, T., & Kato, T. (2021). A review of SWAT model application in  
484 Africa. *Water*, 13(9), 1313.

485 Anaba, L. A., Banadda, N., Kiggundu, N., Wanyama, J., Engel, B., & Moriasi, D. (2016).  
486 Application of SWAT to assess the effects of land use change in the Murchison Bay catchment  
487 in Uganda. *Computational Water, Energy and Env. Engineering*, 6(1), 72868.

488 Arnold, J. G., Srinivasan, R., Muttiah, R. S., & Williams, J. R. (1998). Large area hydrologic  
489 modeling and assessment part I: model development 1. *JAWRA Journal of the American Water*  
490 *Resources Association*, 34(1), 73-89.

491 Arnold, J. G., Moriasi, D. N., Gassman, P. W., Abbaspour, K. C., White, M. J., Srinivasan, R., ...  
492 & Jha, M. K. (2012). SWAT: Model use, calibration, and validation. *Transactions of the*  
493 *ASABE*, 55(4), 1491-1508.

494 Arnold, J. G., Kiniry, J. R., Srinivasan, R., Williams, J. R., Haney, E. B., & Neitsch, S. L. (2013).  
495 SWAT 2012 input/output documentation. Texas Water Resources Institute.

496 Asselman, N. E. M. (2000). Fitting and interpretation of sediment rating curves. *Journal of*  
497 *Hydrology*, 234(3-4), 228-248.

498 Assfaw, A. T. (2019). Calibration, validation and performance evaluation of SWAT model for  
499 sediment yield modelling in Megech reservoir catchment, Ethiopia. *Journal of Environmental*  
500 *Geography*, 12(3-4), 21-31.

501 Assfaw, A. T. (2020). Modeling Impact of Land Use Dynamics on Hydrology and Sedimentation  
502 of Megech Dam Watershed, Ethiopia. *The Scientific World Journal*, 2020, 6530278.

503 Ayalew, L. T., & Bharti, R. (2022). Modeling sediment yield of rib watershed, northwest Ethiopia.  
504 *ISH Journal of Hydraulic Engineering*, 28(sup1), 491-502.

505 Ayana, A. B., Edossa, D. C., & Kositsakulchai, E. (2012). Simulation of sediment yield using  
506 SWAT model in Fincha Watershed, Ethiopia. *Agriculture and Natural Resources*, 46(2), 283-  
507 297.

508 Cousino, L. K., Becker, R. H., & Zmijewski, K. A. (2015). Modeling the effects of climate change  
509 on water, sediment, and nutrient yields from the Maumee River watershed. *Journal of*  
510 *Hydrology: Regional Studies*, 4, 762-775.

511 Dakhlalla, A. O., & Parajuli, P. B. (2019). Assessing model parameters sensitivity and uncertainty  
512 of streamflow, sediment, and nutrient transport using SWAT. *Information Processing in*  
513 *Agriculture*, 6(1), 61-72.

514 Daramola, J., Ekhwan, T. M., Mokhtar, J., Lam, K. C., & Adeogun, G. A. (2019). Estimating  
515 sediment yield at Kaduna watershed, Nigeria using soil and water assessment tool (SWAT)  
516 model. *Heliyon*, 5(7), e02106.

517 Dibaba, W. T., Demissie, T. A., & Miegel, K. (2020). Drivers and implications of land use/land  
518 cover dynamics in Finchaa catchment, northwestern Ethiopia. *Land*, 9(4), 113.

519 Dibaba, W. T., Demissie, T. A., & Miegel, K. (2021). Prioritization of sub-watersheds to sediment  
520 yield and evaluation of best management practices in highland Ethiopia, Finchaa catchment.  
521 *Land*, 10(6), 650.

522 Djebou, D. C. S. (2018). Assessment of sediment inflow to a reservoir using the SWAT model  
523 under undammed conditions: a case study for the Somerville reservoir, Texas, USA.  
524 *International Soil and Water Conservation Research*, 6(3), 222-229.

525 Ebabu, K., Tsunekawa, A., Haregeweyn, N., Adgo, E., Meshesha, D. T., Aklog, D., ... & Yibeltal,  
526 M. (2019). Effects of land use and sustainable land management practices on runoff and soil  
527 loss in the Upper Blue Nile basin, Ethiopia. *Science of the Total Environment*, 648, 1462-1475.



528 Foteh, R., Garg, V., Nikam, B. R., Khadatare, M. Y., Aggarwal, S. P., & Kumar, A. S. (2018).  
529 Reservoir sedimentation assessment through remote sensing and hydrological modelling.  
530 Journal of the Indian Society of Remote Sensing, 46(11), 1893-1905.

531 Franzoia, M., & Nones, M. (2017). Morphological reactions of schematic alluvial rivers: long  
532 simulations with a 0-D model. Int. Journal of Sediment Research, 32(3), 295-304.

533 Gassman, P. W., Reyes, M. R., Green, C. H., & Arnold, J. G. (2007). The soil and water assessment  
534 tool: historical development, applications, and future research directions. Transactions of the  
535 ASABE, 50(4), 1211-1250.

536 Gebretekle, H., Nigusse, A. G., & Demissie, B. (2022). Stream flow dynamics under current and  
537 future land cover conditions in Atsela Watershed, Northern Ethiopia. Acta Geophysica, 70(1),  
538 305-318.

539 Gessese, A., & Yonas, M. (2008). Prediction of sediment inflow to Legedadi reservoir using  
540 SWAT watershed and CCHE1D sediment transport models. Nile Basin Water Engineering  
541 Scientific Magazine, 1, 65-74.

542 Gessesse, B., Bewket, W., & Bräuning, A. (2015). Model-based characterization and monitoring  
543 of runoff and soil erosion in response to land use/land cover changes in the Modjo watershed,  
544 Ethiopia. Land Degradation & Development, 26(7), 711-724.

545 Girmay, G., Moges, A., & Muluneh, A. (2020). Estimation of soil loss rate using the USLE model  
546 for Agewmariayam Watershed, northern Ethiopia. Agriculture & Food Security, 9(1), 1-12.

547 Horowitz, A. J. (2003). An evaluation of sediment rating curves for estimating suspended sediment  
548 concentrations for subsequent flux calculations. Hydrological Processes, 17(17), 3387-3409.

549 Ivanoski, D., Trajkovic, S., & Gocic, M. (2019). Estimation of sedimentation rate of Tikvesh  
550 Reservoir in Republic of Macedonia using SWAT. *Arabian Journal of Geosciences*, 12(14), 1-  
551 13.

552 Jilo, N. B., Gebremariam, B., Harka, A. E., Woldemariam, G. W., & Behulu, F. (2019). Evaluation  
553 of the impacts of climate change on sediment yield from the Logiya Watershed, Lower Awash  
554 Basin, Ethiopia. *Hydrology*, 6(3), 81.

555 Kenea, U., Adeba, D., Regasa, M. S., & Nones, M. (2021). Hydrological responses to land use  
556 land cover changes in the Fincha'a Watershed, Ethiopia. *Land*, 10(9), 916.

557 Khanchoul, K., Amamra, A., & Saaidia, B. (2020). Assessment Of Sediment Yield Using Swat  
558 Model: Case Study Of Kebir Watershed, Northeast Of Algeria. *Big Data In Water Resources*  
559 *Engineering (BDWRE)*, 2, 36-42.

560 Khelifa, W. B., Hermassi, T., Strohmeier, S., Zucca, C., Ziadat, F., Boufaroua, M., & Habaieb, H.  
561 (2017). Parameterization of the effect of bench terraces on runoff and sediment yield by SWAT  
562 modeling in a small semi-arid watershed in Northern Tunisia. *Land Degradation &*  
563 *Development*, 28(5), 1568-1578.

564 Krysanova, V., & White, M. (2015). Advances in water resources assessment with SWAT - an  
565 overview. *Hydrological Sciences Journal*, 60(5), 771-783.

566 Kumar, S., Mishra, A., & Raghuwanshi, N. S. (2012). Estimating catchment sediment yield,  
567 reservoir sedimentation and reservoir effective life using SWAT Model. In *Proceedings of*  
568 *SWAT international conference*, 18-20.

569 Leta, M. K., Demissie, T. A., & Tränckner, J. (2021). Modeling and prediction of land use land  
570 cover change dynamics based on land change modeler (LCM) in Nashe watershed, Upper Blue  
571 Nile basin, Ethiopia. *Sustainability*, 13(7), 3740.

572 Leta, M. K., Demissie, T. A., & Tränckner, J. (2021). Hydrological responses of watershed to  
573 historical and future land use land cover change dynamics of Nashe watershed, Ethiopia. *Water*,  
574 13(17), 2372.

575 Lin, F., Chen, X., Yao, H., & Lin, F. (2022). SWAT model-based quantification of the impact of  
576 land-use change on forest-regulated water flow. *Catena*, 211, 105975.

577 Mariye, M., Mariyo, M., Changming, Y., Teffera, Z. L., & Weldegebrial, B. (2022). Effects of  
578 land use and land cover change on soil erosion potential in Berhe district: a case study of  
579 Legedadi watershed, Ethiopia. *Int. Journal of River Basin Management*, 20(1), 79-91.

580 Megersa, T., Nedaw, D., & Argaw, M. (2019). Combined effect of land use/cover types and slope  
581 gradient in sediment and nutrient losses in Chancho and Sorga sub watersheds, East Wollega  
582 Zone, Oromia, Ethiopia. *Environmental Systems Research*, 8(1), 1-14.

583 Mekuriaw, T. (2019). Evaluating Impact of Land-Use/Land-Cover Change on Surface Runoff  
584 using Arc SWAT Model in Sore and Geba Watershed. *Ethiopia Journal of Environment and  
585 Earth Science*, (10), 7-17.

586 Moriasi, D. N., Wilson, B. N., Douglas-Mankin, K. R., Arnold, J. G., & Gowda, P. H. (2012).  
587 Hydrologic and water quality models: Use, calibration, and validation. *Transactions of the  
588 ASABE*, 55(4), 1241-1247.

589 Neitsch, S. L.; Arnold, J. G.; Kiniry, J. R., et al. (2011). SWAT user manual, version 2009. Texas  
590 Water Resources Institute Technical Report, A&M University, Texas, USA.

591 Negash, D. A., Moisa, M. B., Merga, B. B., Sedeta, F., & Gemedo, D. O. (2021). Soil erosion risk  
592 assessment for prioritization of sub-watershed: the case of Chogo Watershed, Horo Guduru  
593 Wollega, Ethiopia. *Environmental Earth Sciences*, 80(17), 1-11.

594 Pandey, A., Bishal, K. C., Kalura, P., Chowdary, V. M., Jha, C. S., & Cerdà, A. (2021). A soil  
595 water assessment tool (SWAT) modeling approach to prioritize soil conservation management  
596 in river basin critical areas coupled with future climate scenario analysis. *Air, Soil and Water  
597 Research*, 14, 11786221211021395.

598 Pennock, D. (2019). Soil erosion: The greatest challenge for sustainable soil management.  
599 [Policycommons.net](https://www.policycommons.net)

600 Phuong, T. T., Thong, C. V. T., Ngoc, N. B., & Van Chuong, H. (2014). Modeling soil erosion  
601 within small mountainous watershed in central Vietnam using GIS and SWAT. *Resour.  
602 Environ.*, 4(3), 139-147.

603 Qiu, Z., & Wang, L. (2014). Hydrological and water quality assessment in a suburban watershed  
604 with mixed land uses using the SWAT model. *Journal of Hydrologic Engineering*, 19(4), 816-  
605 827.

606 Rathjens, H., & Oppelt, N. (2012). SWAT model calibration of a grid-based setup. *Advances in  
607 Geosciences*, 32, 55-61.

608 Regasa, M. S., Nones, M., & Adeba, D. (2021). A review on land use and land cover change in  
609 Ethiopian basins. *Land*, 10(6), 585.

610 Regasa, M. S., & Nones, M. (2022). Historical and future land use and land cover changes in the  
611 Fincha watershed, Ethiopia. *Land*, 11(8), 1239.

612 Semlali, I., Ouadif, L., Baba, K., Akhssas, A., & Bahi, L. (2017). Using GIS and SWAT model  
613 for hydrological modelling of Oued Laou Watershed (Morocco). *ARNP J. Eng. Appl. Sci.*,  
614 12(23), 6933-6943.

615 Senti, E. T., Tufa, B. W., & Gebrehiwot, K. A. (2014). Soil erosion, sediment yield and  
616 conservation practices assessment on Lake Haramaya Catchment. *World Journal of*  
617 *Agricultural Sciences*, 2(7), 186-193.

618 Setegn, S. G., Dargahi, B., Srinivasan, R., & Melesse, A. M. (2010). Modeling of Sediment Yield  
619 From Anjeni-Gauged Watershed, Ethiopia Using SWAT Model 1. *JAWRA Journal of the*  
620 *American Water Resources Association*, 46(3), 514-526.

621 Sahar, A. A., Hassan, M. A., & Abd Jasim, A. (2021). Estimating the Volume of Sediments and  
622 Assessing the Water Balance of the Badra Basin, Eastern Iraq, Using Swat Model and Remote  
623 Sensing Data. *The Iraqi Geological Journal*, 88-99.

624 Sharma, A., Patel, P. L., & Sharma, P. J. (2022). Influence of climate and land-use changes on the  
625 sensitivity of SWAT model parameters and water availability in a semi-arid river basin. *Catena*,  
626 215, 106298.

627 Swami, V. A., & Kulkarni, S. S. (2016). Simulation of runoff and sediment yield for a Kaneri  
628 Watershed Using SWAT Model. *Journal of Geoscience and Environment Protection*, 4(01), 1.

629 Tefera, B., & Sterk, G. (2010). Land management, erosion problems and soil and water  
630 conservation in Fincha'a watershed, western Ethiopia. *Land Use Policy*, 27(4), 1027-1037.

631 Weldu Woldemariam, G., & Edo Harka, A. (2020). Effect of land use and land cover change on  
632 soil erosion in Erer sub-basin, Northeast Wabi Shebelle Basin, Ethiopia. *Land*, 9(4), 111.

633 Winchell, M., Srinivasan, R., Di Luzio, M., & Arnold, J. (2007). *ArcSWAT interface for SWAT*  
634 *2005. User's Guide*, Blackland Research Center, Texas Agricultural Experiment Station,  
635 Temple.

636 Xue, C., Chen, B., & Wu, H. (2014). Parameter uncertainty analysis of surface flow and sediment  
637 yield in the Huolin Basin, China. *Journal of Hydrologic Engineering*, 19(6), 1224-1236.

- 638 Yasir, M., Hu, T., & Abdul Hakeem, S. (2020). Simulating reservoir induced Lhasa streamflow  
639 variability using ArcSWAT. *Water*, 12(5), 1370.
- 640 Yesuf, H. M., Assen, M., Alamirew, T., & Melesse, A. M. (2015). Modeling of sediment yield in  
641 Maybar gauged watershed using SWAT, northeast Ethiopia. *Catena*, 127, 191-205.
- 642 Yuan, L., & Forshay, K. J. (2019). Using SWAT to evaluate streamflow and lake sediment loading  
643 in the Xinjiang River Basin with limited data. *Water*, 12(1), 39.